New Polymers with Large and Stable Second-Order Nonlinear Optical Effects

Mai Chen, Luping Yu, and Larry R. Dalton*

Department of Chemistry, University of Southern California, Los Angeles, California 90089-1062

Yongqiang Shi and William H. Steier

Center for Photonic Technology, Department of Electrical Engineering, University of Southern California, Los Angeles, California 90089-0483

Received January 2, 1991; Revised Manuscript Received April 8, 1991

ABSTRACT: New polymers containing disperse red dye as a nonlinear optically active chromophore in conjunction with photo-cross-linkable groups have been synthesized. These polymers are soluble in many organic solvents and can be processed into thin films by spin-coating. Second harmonic generation measurements revealed large and stable second-order nonlinear optical effects for these polymers. With the corona poling method, large resonance-enhanced second-order nonlinear optical coefficients were observed at 532 nm. It was found that introduction of flexible chain into the polymer backbone causes a decrease in the T_g value and hence a decrease in the stability of the second-order NLO effects. It was demonstrated that for polymers **2–4**, $\chi^{(2)}$ values are stable at ca. 80–90% of their maximum values for 1000 h after electrical poling. These polymers showed large refractive index changes caused by cis–trans isomerization of azo groups when they are exposed to the UV light. The large refractive index change of these polymers has been utilized in the fabrication of channelized wave-guide structures.

Introduction

Developments of optical communication have led to a tremendous growth in research on nonlinear optical (NLO) materials. Both inorganic and organic materials have been the research focus for NLO applications. Inorganic materials, such as $LiNbO_3$, which have been extensively studied for device applications, have disadvantages such as slow response time, high absorption, and degradative photorefractive effects. These disadvantages limit their application potential.[1] Organic materials, on the other hand, offer advantages of large susceptibilities, high laser damage threshold, faster response time, and versatility of molecular structural modifications.[1-4] Therefore, a growing research effort has been directed to organic materials, among which second-order nonlinear optical polymers have attracted considerable interest in both the industrial and academic communities.[1-12]

Three forms of second-order NLO polymeric materials have been studied: (1) transparent polymers (including liquid-crystal polymers) doped with NLO molecules, i.e., host/guest composite materials;[1-3,10,13,14] (2) polymers covalently functionalized with second-order NLO chromophores[1-3,5,7-9,11,12]; and (3) polymers with covalently attached NLO chromophores and cross-linked after electrical poling.[6] Host/guest polymer composites suffer from limited miscibility of the NLO molecules in host polymers and from the dipole orientation loss due to thermal relaxation. The second type of polymer exhibits much improved stability of NLO activity and a higher density of NLO moieties.[5] The third type of polymer shows even greater stability of the NLO activity than the first two types. Eich et al.[6] found that, in their cross-linked polymers, there was no detectable decay in second harmonic generation for over 500 h under ambient conditions and no relaxation tendency even at 85 °C. Therefore, cross-linkable polymers are promising materials for NLO applications.

Recently we synthesized new second-order NLO polymers containing known NLO moieties with large optical nonlinearities and a cross-linkable unit. A schematic structure of the second-order NLO polymer is shown in Chart I. Schemes I–III show the examples, in which a phenylenediacryloyl chloride monomer is photo-cross-linkable[15] and a diacetylene unit is photo-cross-linkable or thermal cross-linkable.[16] The advantage of these schemes is that many difunctionalized NLO moieties can be incorporated into such polymers. It was found that polymers shown in Schemes I–III demonstrated very large $\chi^{(2)}$ values without exposure to UV light. Furthermore, the second-order NLO effects in these polymer systems (polymers **2–4**) are much more stable than those of normally poled polymers reported in the literature. In contrast to our expectations, it was found that the chromophore in the polymer was bleached when exposed to UV curing light and the $\chi^{(2)}$ value was correspondingly reduced dramatically. These results suggest, on the one hand, that photo-cross-linking results in some trade-off between stability and second-order NLO activity; on the other hand, the large change in the refractive index of polymers that accompanied photobleaching can be utilized in channelized wave-guide fabrication using photomask methods. In this paper we report the syntheses and characterization of these polymer materials.

Experimental Section

Dioxane was purified by distillation over calcium hydride and stored under argon atmosphere. Dimethylacetamide was dried over 3-Å molecular sieves. Pyridine was treated with potassium hydroxide and then distilled over barium oxide to remove trace amounts of water. Terephthaloyl chloride was purified by sublimation under vacuum. Compound **11** was purchased from Aldrich Chemical Co. and was sublimed before use. Other reagents and solvents are analytical-grade quality, purchased commercially, and used without further purification unless otherwise stated. The melting points were obtained with open capillary tubes on a Mel-Temp apparatus and are uncorrected.

Synthesis of Monomers. 1,5-Bis(4-formylphenoxy)pentane (1). A mixture of *p*-hydroxybenzaldehyde (10 g, 0.082 mol), 1,5-dibromopentane (9.42 g, 0.041 mol), potassium carbonate (11.33 g), and potassium iodide (1 g) was heated to reflux in THF (50 mL) overnight and then was poured into water. The yellow precipitate was collected and washed with water. The solid was

0024-9297/91/2224-5421$02.50/0

Chart I
Schematic Structure of a Target New Polymer System

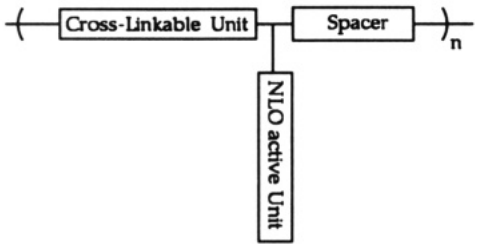

then recrystallized from ethanol to yield compound **1**: 9.3 g, 72%; mp 72–74 °C; ^{1}H NMR (CCl_3D) δ 1.8 (multiple, 6 H, $H_{1,2}$), 4.1 (t, J = 6 Hz, 4 H, H_3), 7.0 (d, J = 9 Hz, 4 H, H_5), 7.8 (d, J = 9 Hz, 4 H, H_6), 9.8 (s, 2 H, H_8); ^{13}C NMR 22.5 (C_1), 29.0 (C_2), 68.0 (C_3), 114.5 (C_5), 129.5 (C_7), 132.0 (C_6), 164.0 (C_4), 170.0 (C_8). Anal. Calcd for $C_{19}H_{20}O_4 \cdot 0.25H_2O$: C, 72.03; H, 6.48. Found: C, 71.98; H, 6.48.

Compound 3. **2**[17a] (6.11 g, 0.029 mol) in ethylene glycol/diethyl ether (10 mL) was added dropwise to ethylene glycol/diethyl ether (20 mL) containing sodium hydride (0.62 g, 0.026 mol). After the completion of the addition, the mixture was stirred for 15 min and compound **1** (4.2 g, 0.013 mol) in THF was then added dropwise. The resulting mixture was stirred at room temperature for 3 h and then poured into water (300 mL). The yellow precipitate was collected and recrystallized from ethanol to yield compound **3**: 3.95 g, 66%; mp 97–99 °C; ^{1}H NMR ($CDCl_3$) δ 1.3 (t, J = 6.0 Hz, 6 H, CH_3), 1.8 (multiple, 6 H, $H_{1,2}$), 4.0 (t, J = 6 Hz, 4 H, H_3), 4.3 (q, J = 6 Hz, 4 H, methylene in ethyl), 6.3 (d, J = 18 Hz, 2 H, H_9), 6.9 (d, J = 9 Hz, 4 H, H_5), 7.5 (d, J = 9 Hz, 4 H, H_6), 7.6 (d, 2 H, J = 18 Hz, H_8). Anal. Calcd for $C_{27}H_{32}O_6$: C, 71.68; H, 7.08. Found: C, 71.60; H, 7.15.

Compound 4. **3** (3.68 g, 8.14 mmol) was heated to reflux with sodium hydroxide (1.0 g) in ethanol/water (60/40 v/v, 50 mL) for 1 h. The mixture was then treated with 5 N hydrogen chloride acid. The solid was washed with water until the filtrate become neutral, yielding compound **4**: 2.90 g, 90%; mp 271–273 °C; ^{1}H NMR (DMSO-d_6) δ 1.7 (br, 6 H, $H_{1,2}$), 4.0 (t, J = 6 Hz, 4 H, H_3), 6.4 (d, J = 18 Hz, 2 H, H_9), 6.9 (d, J = 9 Hz, 4 H, H_5), 7.5 (d, J = 9 Hz, 4 H, H_6), 7.6 (d, 2 H, J = 18 Hz, H_8). Anal. Calcd for $C_{23}H_{24}O_6$: C, 69.70; H, 6.06. Found: C, 69.56; H, 6.09.

Compound 5. **4** (2 g, 5.06 mmol) was heated to reflux with thionyl chloride (10 mL) and benzene (2 mL). After 1 h, the while solid was completely dissolved and the thionyl chloride was then removed by distillation. A trace amount of residual thionyl chloride was removed by vacuum pumping yielding compound **5**, which is directly used in the next polymerization step.

***p*-Phenylenediacrylic acid (7).** This compound was prepared according to a literature procedure in 87% yield (mp >400, sublimation).[17b] The white solid has to be extracted with chloroform to remove a small amount of monoacrylic acid: ^{1}H NMR (DMSO-d_6) δ 6.55 (d, 2 H, OCCH=, J = 15 Hz), 7.57 (d, 2 H, =CHPh, J = 15 Hz), 7.69 (s, 4 H, aromatic). Anal. Calcd for $C_{12}H_{10}O_4$: C, 66.06; H, 4.59. Found: C, 65.89; H, 4.65.

***p*-Phenylenediacryloyl chloride (8).** **7** (2 g, 9.17 mmol) was heated to reflux with thionyl chloride (10 mL) and benzene (2 mL). After 1 h, the white solid was completely dissolved and the thionyl chloride was then removed by distillation. A trace amount of residual thionyl chloride was removed by vacuum pumping. The yellow solid obtained was further purified by sublimation under vacuum, yielding compound **8** (2.14 g, 91%).

2,2′-[4-[(4-Nitrophenyl)azo]phenyl]iminobisethanol (6, Disperse Red 19). p-Nitroaniline (6.9 g, 50 mmol) was dissolved in 18% hydrochloride solution (30 mL) and diazotized with sodium nitrite (3.45 g in 5 mL of H_2O, 50 mmol) at 0–5 °C. The mixture was then added dropwise to bis(hydroxyethyl)aniline (8.9 g, 50 mmol) in concentrated hydrochloride solution (25 mL) at 0–5 °C. The mixture was stirred for another 1 h, and saturated sodium acetate solution was then added to neutralize the mixture. The deep red precipitate was collected and washed several times with water. Recrystallization from ethanol gave compound **6**: 13.53, 82%; mp 198–200 °C; ^{1}H NMR (DMSO-d_6) δ 3.6 (s, 8 H, CH_2), 4.90 (s, 2 H, OH), 6.9 (d, 2 H, H_e, J = 15 Hz), 7.8 (d, 2 H, H_g, J = 15 Hz), 7.9 (d, 2 H, H_f, J = 15 Hz), 8.3 (d, 2 H, H_h, J = 15 Hz); the numbering of the protons is shown in Scheme I. Anal. Calcd for $C_{16}H_{18}N_4O_4$: C, 58.16; H, 5.50; N, 16.96. Found: C, 58.00; H, 5.48; N, 16.99.

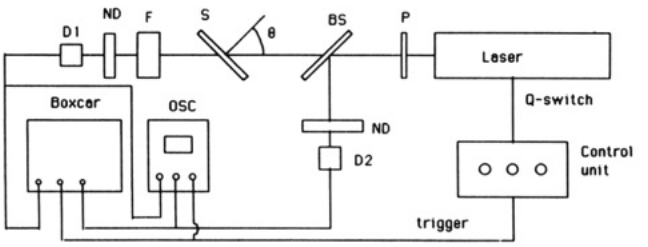

Figure 1. Schematic diagrams of second harmonic generation experimental setup. Key: P, polarizer; BS, beamsplitter; S, sample polymer film; F, fundamental wavelength filter; ND, neutral density filter; D1, D2, detectors; OSC, oscilloscope; Boxcar, boxcar integrator.

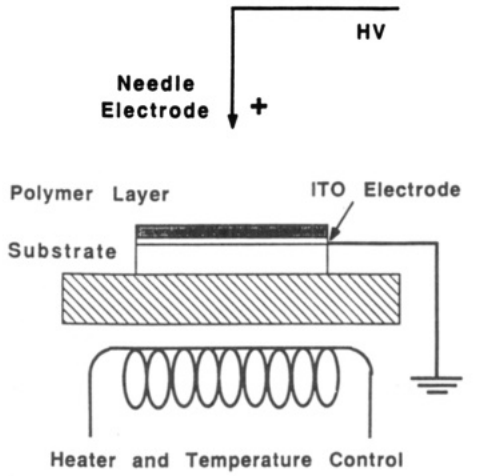

Figure 2. Corona poling setup used in poling polymer thin films.

Syntheses of Polymers. Polymer 1. The above compounds **5** and **6** (1.67 g, 5.06 mmol) were dissolved in dioxane (15 mL), and pyridine (0.5 mL) was added to the solution. The mixture was heated to reflux for 2 h under an argon atmosphere. The resulting polymer solution was poured into ethanol (20 mL), and the polymer precipitate was collected by filtration and washed with ethanol. The polymer was further purified by extraction in a Soxhlet extractor with ethanol and dried under vacuum overnight, yielding polymer **1**: 3.1 g, 88%. Anal. Calcd for $C_{39}H_{38}N_4O_8$: C, 67.82; H, 5.51; N, 8.12. Found: C, 66.64; H, 5.57; N, 8.00.

Polymer 2. **8** (0.5 g, 1.96 mmol) and **6** (0.647 g, 1.96 mmol) were dissolved in dioxane (15 mL) and pyridine (0.5 mL) was added to the solution. The mixture was heated to reflux for 2 h under an argon atmosphere. The resulting polymer solution was poured into ethanol (20 mL), and the polymer precipitate was collected by filtration and washed with ethanol. The polymer was further purified by extraction in a Soxhlet extractor with ethanol and dried under vacuum overnight, yielding polymer **2**: 0.94 g, 94%. Anal. Calcd for $(C_{28}H_{24}N_4O_6)_n$: C, 65.63; H, 4.69; N, 10.94. Found: C, 64.42; H, 4.82; N, 10.79.

Polymer 3. Terephthaloyl chloride (1.93 g, 9.50 mmol) dissolved in dichloroethane (10 mL) was added dropwise to the mixture containing 1,6-dihydroxy-2,4-hexidiyne[18] (0.524 g, 4.75 mmol), **6** (1.569 g, 4.75 mmol), dichloroethane (10.0 mL), and pyridine (3.0 mL). The resulting mixture was heated to 70 °C for 2 h and was then poured into ethanol. The polymer precipitate was collected and handled as for polymer **1**: 3.32 g, 90%. Anal. Calcd for $(C_{38}H_{28}N_4O_{10})_n$: C, 65.14; H, 4.00; N, 8.00. Found: C, 64.39; H, 4.14; N, 7.85.

Polymer 4. The mixture of **11** (1.35 g, 4.55 mmol) and **6** (1.50 g, 4.55 mmol) in dimethylacetamide (20 mL) was heated to 100 °C for 2 h and was then poured into ethanol (50 mL). The precipitate was collected and washed with ethanol. The polymer was further purified by extraction in a Soxhlet extractor with

ethanol to yield polymer 4: 2.60 g, 91%. Anal. Calcd for $C_{32}H_{30}N_6O_8$: C, 61.33; H, 4.83; N, 13.40. Found: C, 60.79; H, 5.01; N, 13.36.

Characterization of Monomers and Polymers. FTIR spectra were taken as pressed KBr pellets or polymer films cast on a sodium chloride crystal disk with a 1760 Perkin-Elmer FTIR spectrometer. UV/vis spectra were obtained on a Perkin-Elmer Lambda 4C UV/vis spectrophotometer. NMR spectra were recorded on JEOL FX-90 Q FT NMR or on a Bruker AC 250-MHz FT NMR spectrometer. Thermal analyses were performed using Perkin-Elmer DSC-7 and TGA-7 systems with a heating rate of 20 °C/min. Viscosity measurements were performed employing a Ubbelohde viscometer.

NLO Measurements. Second-order nonlinear optical properties such as the second-order nonlinear susceptibility tensor elements χ_{ijk}, second harmonic generation coefficients d_{ijk}, and electrooptic coefficients r_{ijk} are related to each other through the following equations.[8]

$$d_{ijk} = \frac{1}{2}\chi_{ijk}^{(2)} \tag{1}$$

and

$$d_{ijk} = -(n_i^2 n_j^2/4) r_{ijk} \tag{2}$$

where n is the refractive index of the nonlinear material. At fundamental frequency ω differing from that of the measurements, ω', these nonlinear coefficients can be deduced from their dispersion relations on the basis of a simple two-level model.[8] The second harmonic generation coefficient can be expressed as

$$d_{ijk}(2\omega,\omega,\omega) = d_{ijk}(2\omega',\omega',\omega')\frac{f^{2\omega}(f^{\omega})^2}{f^{2\omega'}(f^{\omega'})^2}\frac{(\omega_0^2-\omega'^2)(\omega_0^2-4\omega'^2)}{(\omega_0^2-\omega^2)(\omega_0^2-4\omega^2)} \tag{3}$$

and the electrooptic coefficient at frequency ω'' as

$$r_{ijk}(\omega,\omega,0) = -\frac{4d_{kij}}{n_i^2(\omega)n_j^2(\omega)}\frac{f_{ii}^{\omega}f_{jj}^{\omega}f_{kk}^{0}}{f_{kk}^{2\omega'}f_{ii}^{\omega'}f_{jj}^{\omega'}}\frac{(3\omega_0^2-\omega^2)(\omega_0^2-\omega'^2)(\omega_0^2-4\omega'^2)}{3\omega_0^2(\omega_0^2-\omega^2)^2} \tag{4}$$

where ω_0 is the frequency of the resonance peak; ω' is the fundamental frequency used in measuring d_{ijk}, ω and ω'' are the frequencies of interest, and f's are the local field factors.

The second harmonic measurements were performed utilizing the setup shown in Figure 1. A Spectra-Physics DCR-11 Q-switched Nd:YAG laser with pulse width of <10 ns and 10-Hz repetition rate was used as a fundamental source. The polymers were dissolved in chloroform and filtered through a 0.2-μm filter. The filtered solutions were spin-cast on transparent glass substrates with an ITO conductive layer as the poling electrode. The polymer films were dried either by baking polymer films at 90 °C for 10 min or leaving under ambient conditions for 2 days. Since the polymer films were very thin, there should be no chloroform residue in the films after these treatments. Experiments showed that both procedures gave identical results. The polymer film thickness ranged from several hundred to several thousand angstroms as measured with an Rudolph 43603-200E ellipsometer and a Dektak II profiler. The dried film was then heated to near or above its glass transition temperature T_g and corona poled with an intense dc electrical field, as shown in Figure 2. The poling conditions are as follows: temperature, 120–130 °C; high voltage, 12–14 kV at needle point; poling time, ~2 min; gap distance, ca. 1.5 cm; poling current, <0.1 mA. The polymer film was cooled to room temperature in the presence of an electrical field.

The polymer sample was held at a 45° angle to the incident laser beam with the polarization of the beam in the incident plane. The second harmonic signals were detected by a photomultiplier and averaged over 300 pulses with a boxcar integrator. A crystal quartz sample with known thickness and d coefficient was used as reference. The second harmonic coefficients of the polymer films were calculated by comparing their second harmonic intensity with that generated by the quartz sample, with the assumption that $d_{33} = 3d_{13}$.[19] The substrate (conducting ITO glass) contribution to the second harmonic signal, ~3 orders less than that of polymer films, was negligible.

Scheme I
Synthesis of Polymer 1

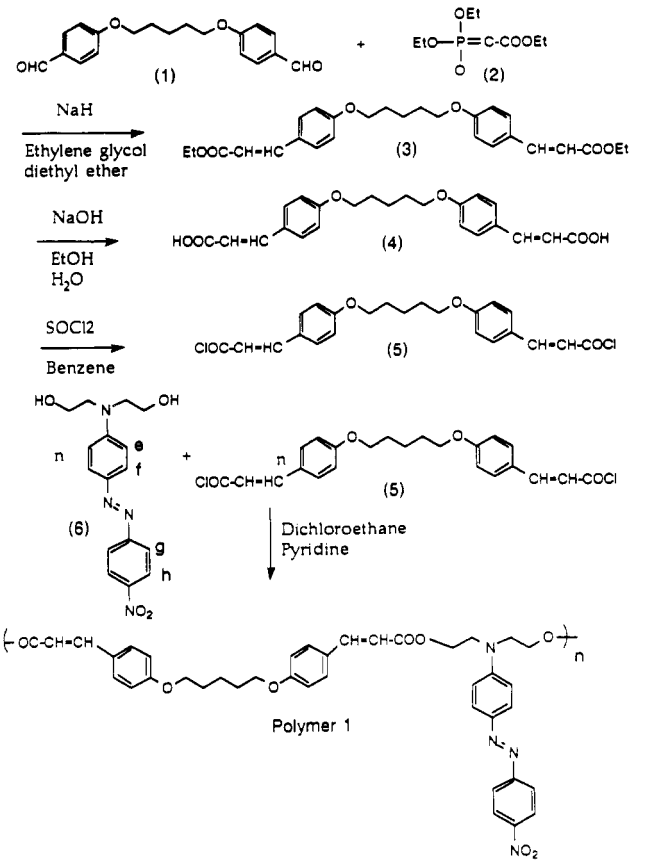

Results and Discussion

Syntheses of Monomers. Monomer 5 is prepared by a three-step reaction scheme (see Scheme I) starting from compound 1. We attempted to react 1 with malonic acid in pyridine. A mixture containing monoacrylic acid was obtained, which was difficult to purify. The approach shown in Scheme I, in which a Wittig reaction has been employed, yields pure monomers. 3 can be synthesized in a relatively high yield, which is easy to purify and convert into monomer 5. Synthesis of monomer 6 is easily effected by using diazo coupling reaction. To prepare monomer 8, we chose a simple approach as shown in Scheme II, in which terealdehyde is reacted with malonic acid in ethanol with piperidine and pyridine as catalysts. The final products contain a small amount of monoacrylic acid, which can be removed by extraction with chloroform.

Synthesis of Polymer. Since disperse red dyes showed large second-order NLO effects,[20] we utilized the difunctionality of disperse red 19 to prepare linear polymers. The initial aim of this work was to synthesize cross-linkable second-order NLO polymers. Chart I shows the target new polymers containing NLO chromophores, cross-linkable units and a flexible chain, the length of which can be varied to adjust the glass transition temperature of the resulting polymers. An example is shown in Scheme I where monomer 5, containing acryloyl chloride groups and a flexible chain, is polymerized with disperse red 19 to prepare polymer 1. Since the cinnamic group is a well-known photo-cross-linkable unit,[15] polymer 1 is expected to be a photo-cross-linkable second-order NLO polymer. Using monomer 8 without a flexible chain segment, we prepared polymer 2 (see Scheme II), which is also photo-cross-linkable, and physical studies indicate that this polymer possesses more interesting properties than poly-

Scheme II
Synthesis of Polymer 2

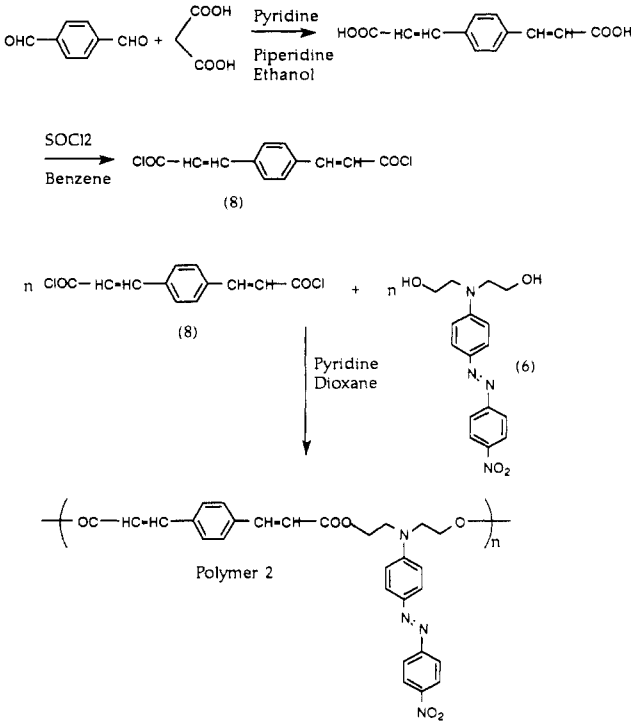

Scheme III
Synthesis of Polymer 3

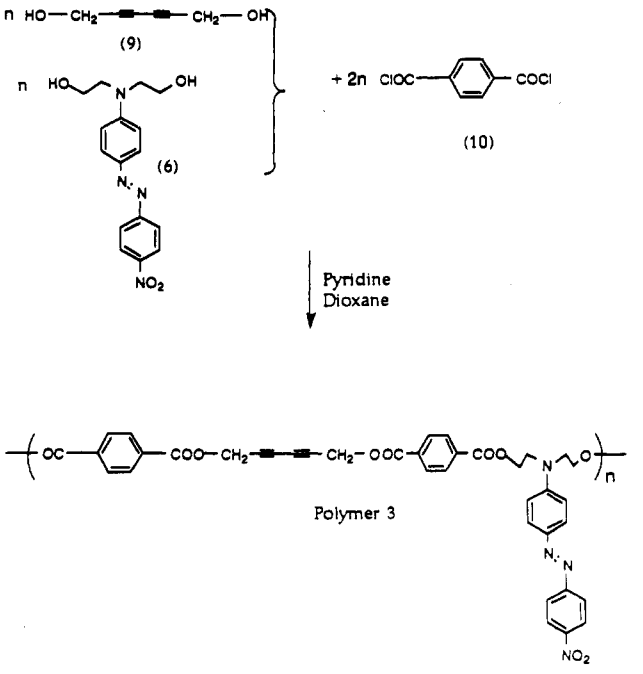

mer 1, as will be shown below. Another approach for preparing cross-linkable polymers is based on the observation that diacetylenes can be polymerized by heat or light initiation. If diacetylene can be incorporated into the polymer backbone, a cross-linkable site is then introduced into the polymer. Therefore, we chose the diacetylene as comonomer in the synthesis of copolymer 3, as shown in Scheme III. All of these polymerizations were carried out in dioxane or dichloroethane. For comparison, we synthesized polymer 4 without cross-linkable units, as shown in Scheme IV. The polymers obtained are all partially soluble in chloroform, THF, DMSO, and DMF and are soluble in *m*-cresol and *N*-methylphthalimide. Optical quality films can be cast by using the spin-coating

Scheme IV
Synthesis of Polymer 4

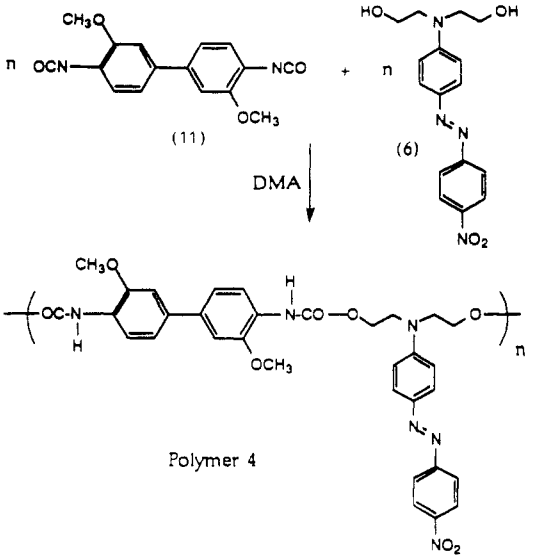

Table I
Physical Properties of Polymers 1–4

polymers	$[\eta]$,[a] dL/g	T_g, °C	T_m, °C	λ_{max},[b] nm
1	0.30	92	120	460
2	0.17	120	190	470
3	0.27	122		455
4	0.20	140		463

[a] *N*-Methylpyrrolidone is solvent. [b] The value in visible region.

technique. Viscosity measurements show that these polymers have an intrinsic viscosity around 0.2 dL/g as shown in Table I. Elemental analysis results fit the polymer structures drawn in Schemes I–IV.

Characterization of Polymer. Figure 3 shows ^1H NMR spectra of polymers 1–4, in which the assignments are consistent with the structures drawn. For polymers 1–4, the chemical shifts of the methylene group in the disperse red 19 unit appear at 3.8 and 4.5 ppm, respectively. The spectrum of polymer 1 shows the chemical shifts of a flexible chain at 1.6, 1.8, and 4.0 ppm. The chemical shifts due to vinyl protons of polymers 1 and 2 appear at 6.3 and 7.6 ppm with multiple peaks, which could be due to an end-group effect. The spectrum of polymer 3 shows a methylene ($OCH_2C{=}C$) chemical shift at 5.0 ppm, which has the same integration area as those for either OCH_2 or NCH_2 and provides further support for the polymer composition drawn in Scheme III. The methyl chemical shift in polymer 4 appears to be overlapped with the methylene group in NCH_2 at 3.85 ppm. The assignments of all other chemical shifts according to the expected structures are indicated in Figure 3.

FTIR spectra of polymers 1–4 are shown in Figure 4, in which absorptions due to nitro groups can be observed around 1520 and 1350 cm^{-1}. For polymers 3 and 4, the carbonyl absorptions appear at 1730 cm^{-1}, while the carbonyl absorptions in polymers 1 and 2 appear at 1720 cm^{-1} due to conjugation with vinyl group. The absorption band due to the vinyl group in polymer 1 is around 990 cm^{-1} and the absorption due to the diacetylene unit in polymer 3 appears around 2200–1950 cm^{-1}. A sharp absorption at 3435 cm^{-1} for polymer 4 due to NH can be observed.

The thermal properties of these polymers have been studied by employing DSC and TGA. Figure 5 shows DSC traces for these polymers from which T_g values can be deduced and are listed in Table I. It can be noted that the glass transition temperature of polymer 1 is lower than

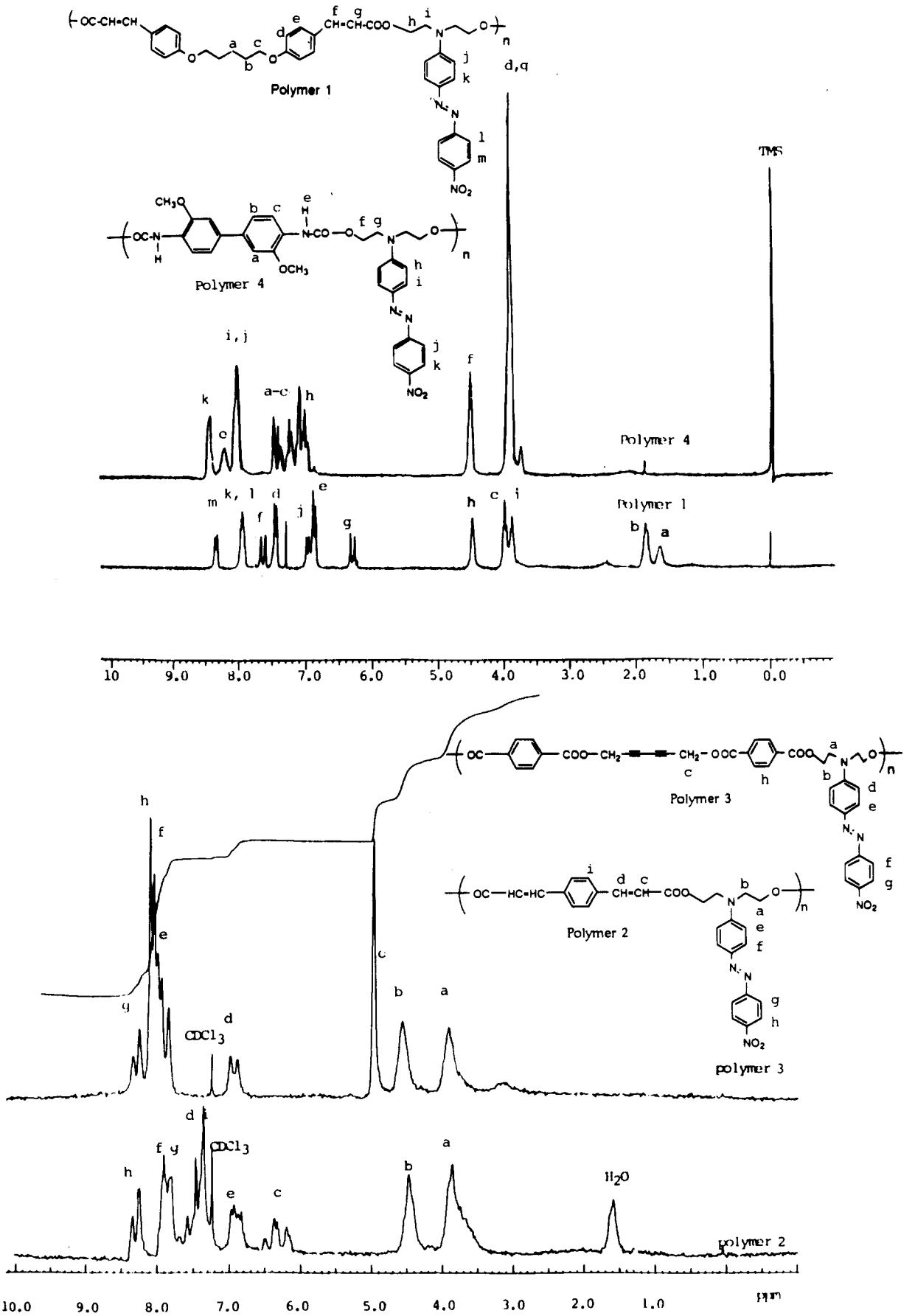

Figure 3. ^{1}H NMR spectra of (a, top) polymers 1 and 4 and (b, bottom) polymers 2 and 3 (in $CDCl_3$).

the others, which obviously is caused by introduction of the flexible chain segment. In polymer 4, there is hydrogen bonding due to the imide units, which increases the glass transition temperature. The differences in T_g of these polymers have been reflected in the electrically poling dynamics, as will be discussed below. For polymers 1 and 2, melting transitions were observed at 120 and 183 °C, respectively, which have been supported by melting process

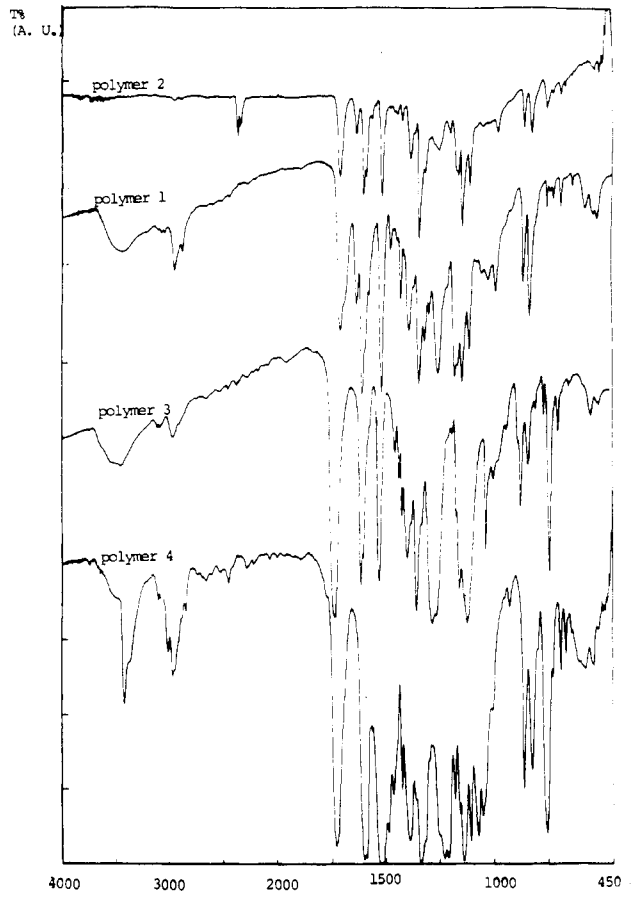

Figure 4. FTIR spectra of polymers 1–4.

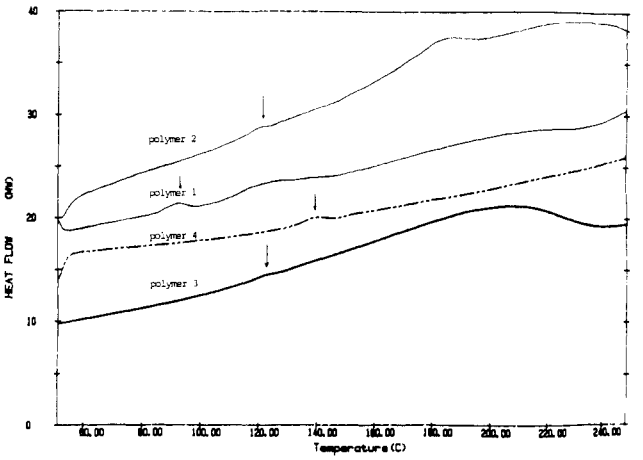

Figure 5. Diagrams of DSC trace of polymers 1–4.

observations and TGA data. When the polymers were heated in a melting tube, the molten state was observed at around 120 °C for polymer 1 and 190 °C for polymer 2, and the TGA trace of polymer 2 shows no weight loss until 250 °C. For polymer 3, the process at 200 °C is a much broader, exothermic process and might involve more complicated process. TGA data show slight weight loss starting at 200 °C and a fast decomposition at 250 °C. Polymer 4 shows no thermal process other than glass transition at 140 °C in the DSC trace between 60 and 240 °C.

Linear Optical Properties. UV/vis spectra of the polymers, measured in thin films, show absorptions in the visible region, which is summarized in Table I. The difference in the absorption of these polymers is due to the difference in polymer backbone structures. Polymers 1–3 have been tested for photoinduced cross-linking using

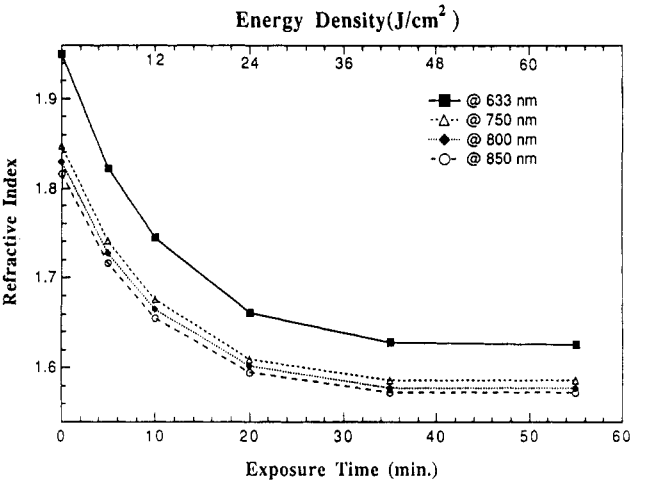

Figure 6. Refractive indices as a function of exposure time to UV light for polymer 2, exposed by Karl Suss mask aligner (12 mW/cm² at 405 nm and 6 mW/cm² at 365 nm).

a mercury lamp as UV light source. We observed a photobleaching process in all these polymer systems. For example, polymer 2 is transparent from 640 nm to the near-infrared region. When polymer thin films are exposed to UV light, photobleaching occurs. Figure 6 is a plot of refractive indices measured from four-zone average ellipsometry at different wavelengths as a function of exposure time. It can be seen that as the exposure time increased, the film index decreased rapidly at low exposure level and saturated at high exposure dose. After 40 min of exposure, the refractive index then achieved a stable value and an overall refractive index decrease of $\Delta n > 0.3$ at 633 nm in the exposed area was recorded. Solubility change has been observed for UV light exposed polymer thin films; the spot exposed cannot be washed out with chloroform while the area unexposed can be redissolved in chloroform. FTIR spectra detected a decrease in the intensity of vinyl proton absorption in polymer 2 after exposure, which is a good indication of photo-cross-linking; however, the change is too small to permit quantitative calculation of cross-linking density. Furthermore, second harmonic generation measurements showed a considerable decrease in second-order NLO coefficients for these polymers after exposure. A reduction of 90% in d_{33} was observed for poled sample after a 40-min exposure. These refractive index changes and decreases in second-order NLO effects are mainly due to photoinduced cis–trans isomerization of the azo unit in NLO chromophores. This isomerization was demonstrated in Figure 7, where all of the spectra curves were plotted at same base-line setting. As the exposure dose increased, more trans isomer changed to the cis form and the absorption peak decreased. Further studies showed that after thermal annealing at 80 °C for polymer 1 and 140 °C for polymers 2–4 we could only partly recover the reduced refractive index and second-order NLO activities, which suggests that the cross-linked polymer matrix might hinder cis–trans isomerization.

Although photobleaching reduces the NLO effect, the large index change of these polymers can be utilized in device fabrication. For example, it is possible to define channel wave-guide structures and other patterns simply by using a photomask and a conventional semiconductor device processing mask aligner. We have succeeded in fabrications of primary wave-guide structures. Detailed results will be reported elsewhere and will not be discussed in this paper.[21]

NLO Properties. The second-order optical nonlinearity of these polymers has been characterized via second

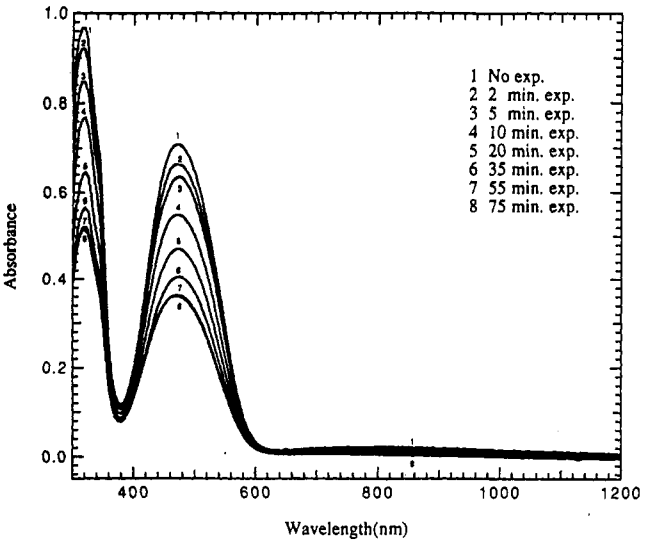

Figure 7. UV/vis absorption spectrum change at different UV exposure dose levels.

Table II
NLO Properties of Polymers 1–4

polymer	d_{33}, pm/V (stabilized)	$\chi^{(2)}$, 10^{-7} esu	r_{33}, pm/V	chromophore density,[a] %	sample thickness, μm
1	108	5.15	23	48	0.04
2	250	12.70	26	68	0.05
3	119	5.68	24	47	0.22
4	223	10.65	22	52	0.28

[a] $C_{16}H_{16}N_4O_4$ has been taken as the formula of the chromophores.

harmonic generation (SHG). From measured second harmonic output, thin-film refractive indices, thickness, and absorbance at second harmonic wavelength, the magnitude of the SHG coefficients were calculated by comparing with quartz reference signal.[19] The angular dependence pattern of the second harmonic signal was similar to that reported in ref 19 because the film thicknesses were very small. Since the second harmonic wavelength was about 60–70 nm away from the resonance peak, the coherence length became complex and therefore the absorption of polymer samples were included in the calculation.[22,23] The obtained stabilized d_{33} values at 1064-nm fundamental wavelength are listed in Table II. The measurement errors were estimated ~25%, including 10% uncertainty of quartz reference. These d_{33} values can be converted to $\chi^{(2)}$ values by using eq 1; thus, $\chi^{(2)}$ values of polymers 1–4 are also listed in Table II. These polymer materials (polymers 2–4) showed a high stability in second-order NLO effect without exposure to UV light. Figure 8 shows the temporal behavior of the second harmonic coefficients of polymers 1–4. It can be seen that polymer 1 has poorer stability than polymers 2–4. The second harmonic coefficients, $d_{33}(t)$, of polymer 1 decayed rapidly to 40% within 100 h and then stabilized at 40% of their maximum value. The reason for this fast decay is due to the lower glass transition temperature, ca. 90 °C, which is caused by introduction of the flexible chain. For polymers 2 and 3, the second harmonic coefficients, $d_{33}(t)$, were stabilized at 80–90% of their initial values, $d_{33}(0)$. The difference between these two polymers in the stability of the d_{33} values might be due to a different polymer backbone because the phenylenediacrylic unit in polymer 2 is more rigid than the diacetylene unit in polymer 3. In polymer 4, there exists hydrogen bonding, which plays the cross-linking role so that the dipole orientation after electrically poling can be stabilized.

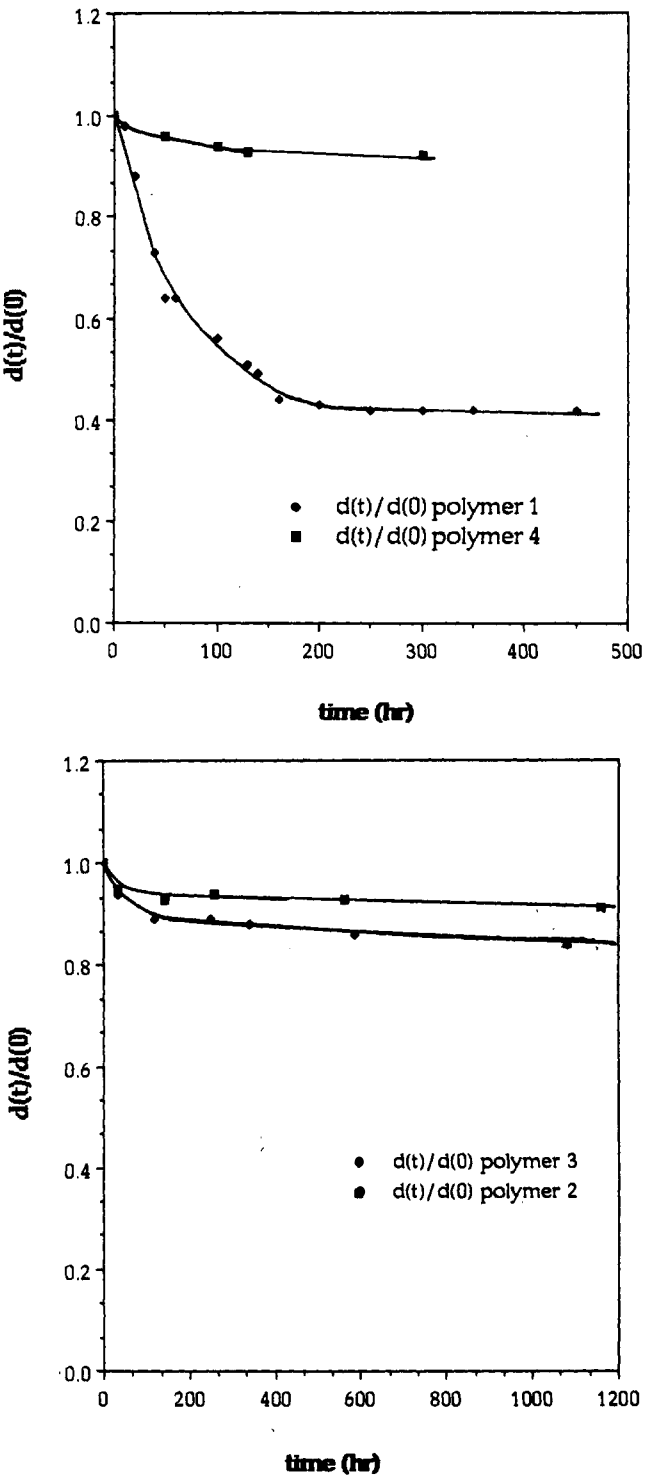

Figure 8. Temporal behavior of second harmonic coefficients of (a, top) polymers 1 and 4 and (b, bottom) polymers 2 and 3.

Comparing these polymers with those doped with NLO molecules and those covalently functionalized with NLO moieties,[5,6] we note that the $d_{33}(t)$ values of these polymers are sizable, stable second-order coefficients reported in the literature. The difference in $d_{33}(t)$ values (see Table II) for these polymers is related to the difference in chromophore density and the difference in resonant enhancements. If we take $C_{16}H_{16}N_4O_4$ as the formula of the chromophore, the weight percentages of the chromophore in polymers 1–4 are listed in Table II. Polymer 2 has highest density of chromophores and its absorption peak in the visible region (470 nm) is closer to second harmonic frequency than other polymers; therefore, polymer 2 has the largest resonance-enhanced d_{33} value. Polymers 1 and

3 have lower chromophore density; their stabilized $d_{33}(t)$ are smaller than other polymers. Polymer 4 has high chromophore density; its absorption is closer to second harmonic frequency and hence it has larger resonant enhancement than polymers 1 and 3. Therefore, polymer 4 possesses a higher d_{33} value than polymers 1 and 3. Of course, we have not taken molecular interaction, which might have a significant contribution to the NLO effect, into consideration in the above discussion.

For integrated optical applications, semiconductor lasers are the major light sources and transparent electrooptic materials are usually used. Hence, the second-order NLO coefficients near-infrared wavelength are more important. By use of a simple two-level model, the measured d_{33} values were extrapolated to 800-nm (near-infrared) wavelength, where the polymer films are transparent, to obtain the electrooptic coefficient r_{33} (electronic contribution) from eqs 3 and 4. The results are summarized in Table II, from which we note that the r_{33} values for all these materials are similar; this is additional evidence supporting the statement above about resonant enhancement. It should be noted that this extrapolation was simply for comparison purposes since the damping effect or the line width of the dispersion has not been taken into consideration, although the second harmonic wavelength was quite close to the resonance peak. However, neglect of the line width should result in, mathematically, an underestimation of the nonlinear coefficients at longer wavelength. Detailed measurements of electrooptical coefficients of these polymers at longer wavelengths are in progress and will be reported later.

As mentioned above, photo-cross-linking resulted in a decrease of second-order NLO effects. After thermal annealing under vacuum at 70–80 °C, we are able to partially recover the second-order NLO effects. Detailed studies will be presented elsewhere.[24]

Conclusion

Linear polymers containing dispersed red dye and cross-linkable groups have been synthesized. These polymer systems have very high chromophore density and large solubility in normal organic solvents. These polymeric materials without exposure to UV curing light exhibit very large and stable second-order NLO activities. In comparison with those doped with NLO molecules and those covalently functionalized with NLO moieties, the $\chi^{(2)}$ values of these polymers are more promising in practical applications. Another feature of these polymer systems is the large photoinduced refractive index change, which has been utilized in the preparation of channel wave-guide structures.

Acknowledgment. This work was supported by Air Force Office of Scientific Research Contracts F49620-87-C-0100 and F49620-88-C-0071 and by the National Science Foundation under Grant DMR-88-15508.

References and Notes

(1) Williams, D. J., Ed. *Nonlinear Optical Properties of Organic and Polymeric Materials*; ACS Symposium Series 233; American Chemical Society: Washington, DC, 1983.
(2) Messier, J., Kajzar, F., Prasad, P., Ulrich, D., Eds. *NATO ASI Ser., Ser. E.* **1989**, *No. 162.*
(3) Khanarian, G. Ed. Molecular and Polymeric Optoelctronic Materials: Fundamentals and Applications. *Proc. SPIE Int. Soc. Opt. Eng.* **1986**, *682.*
(4) Heeger, A. J.; Orenstein, J.; Ulrich, D. R. Nonlinear Optical Properties of Polymers. *Mater. Res. Soc. Symp. Proc.* **1988**, *109.*
(5) (a) Ye, C.; Minami, N.; Marks, T. J.; Yang, J.; Wong, G. K. *Macromolecules* **1988**, *21*, 2899. (b) Ye, C.; Marks, T. J. *Macromolecules* **1987**, *20*, 2322.
(6) Eich, M.; Reck, B.; Yoon, D. Y.; Willson, C. G.; Bjorklund, G. C. *J. Appl. Phys.* **1989**, *66*, 3241.
(7) Robello, D. R. *J. Polym. Sci., Polym. Chem. Ed.* **1990**, *28*, 1.
(8) Singer, K. D.; Sohn, J. E. In *Elecroresponsive Molecules and Polymeric Systems*; Skotheim, T. A., Ed.; Marcel Dekker Inc.: New York, 1991; Vol. 2, Chapter 2, p 49.
(9) Hill, J. R.; Panties, P.; Abbasi, F.; Hodge, P. *J. Appl. Phys.* **1988**, *64*, 2749.
(10) Singer, K. D.; Lalama, S. J.; Sohn, J. E. *Proc. SPIE Int. Soc. Opt. Eng.* **1985**, *578*, 130.
(11) Eich, M.; Sen, A.; Looser, H.; Yoon, D. Y.; Bjorklund, G. C.; Tweig, T.; Swalen, J. P. In Nonlinear Optical Properties of Organic Materials; Khanarian, G., Ed.; SPIE: Bellingham, WA, 1988; Vol. 971, p 128.
(12) Singer, K. D.; Kuzyk, M. g.; Holland, W. R.; Sohn, J. E.; Lalama, S. J.; Comizzoli, R. B.; Katz, H. E.; Schiling, M. L. *Appl. Phys. Lett.* **1988**, *53*, 1800.
(13) Meredith, G. R.; VanDusen, J. G.; Williams, D. J. *Macromolecules* **1982**, *15*, 1385.
(14) Hampsch, H. L.; Yang, J.; Wong, G. K.; Torkelson, J. M. *Macromolecules* **1988**, *21*, 526.
(15) (a) Stobbe, H. *Ber. Dtsch. Chem. Ges.* **1919**, *52B*, 666. (b) Hasegawa, M. In *Comprehensive Polymer Science*; Allen, G., Bevington, J. C., Eds.; Pergamon Press: New York, 1989; Vol. 5, p 217.
(16) (a) Bloor, D. In *Comprehensive Polymer Science*; Allen, G., Bevington, J. C., Eds.; Pergamon Press: New York, 1989; Vol. 5, p 233. (b) Yu, L. P.; Chen, M.; Dalton, L. R. *J. Polym. Sci., Polym. Lett. Ed.*, in press.
(17) (a) Wolinsky, J.; Erickson, K. L. *J. Org. Chem.* **1965**, *30*, 2208. (b) Ruggli, Theilheimer, W. *Helv. Chim. Acta* **1941**, *24*, 899.
(18) Milas, N. A.; Mageli, O. L. *J. Am. Chem. Soc.* **1963**, *75*, 5970.
(19) Mortazavi, M. A.; Knoesen, A.; Kowel, S. T.; Higgins, B. G.; Dienes, A. *J. Opt. Soc. Am.* **1989**, *B6*, 733.
(20) Singer, K. D.; Sohn, J. E.; King, L. A.; Gordon, H. M.; Katz, H. E.; Dirk, C. D. *J. Opt. Soc. Am.* **1989**, *B6*, 1339.
(21) Shi, Y. Q.; Steier, W. H.; Yu, L. P.; Chen, M.; Dalton, L. R. *Appl. Phys. Lett.*, in press.
(22) Shen, Y. R. *The Principles of Nonlinear Optics*; John Wiley & Sons: New York, 1984; Chapter 6.
(23) Dick, B.; Hochstrasser, R. M.; Trommsdorff, H. P. In *Nonlinear Optical Properties of Organic Molecules and Crystals*; Chemla, D. S., Zyss, J., Eds.; Academic Press: Orlando, FL, 1987; Vol. II, p 159.
(24) Cao, S.; Yu, L. P.; Dalton, L. R., submitted to *J. Appl. Phys.*

Registry No. (5)(6) (copolymer), 134847-51-1; (5)(6) (SRU), 134847-48-6; (6)(7) (copolymer), 134847-54-4; (6)(7) (SRU), 134847-49-7; (6)(8) (copolymer), 134847-52-2; (6)(8) (SRU), 133926-54-2; (6)(9)(10) (copolymer), 134847-53-3.